J Therm Anal Calorim (2010) 100:1017–1025
DOI 10.1007/s10973-009-0615-1

Thermal studies of DBSA-doped polyaniline/PVC blends by isothermal microcalorimetry

Asma Binat Afzal · Muhammad Javed Akhtar · Lars-Gunnar Svensson

Received: 16 April 2009 / Accepted: 18 November 2009 / Published online: 2 December 2009

Abstract A series of blends of dodecylbenzenesulfonic acid (DBSA)-doped polyaniline (PANDR) and PVC were synthesized by solution blending technique and investigated by heatflow microcalorimetry (HFC) for thermal and oxidative stability and for PVC–PANDR compatibility. FTIR results provided evidence for strong dipole–dipole interactions between PANDR and PVC. The energy of the oxidation is independent of the composition. The interaction energy and thermal stability increased with the increase of PANDR content in the blend. The activation energies calculated by using Arrhenius relationship can be employed for accelerated ageing of the synthesized blends. It has been observed that the average degradation of PANDR component is higher than that of PVC.

Keywords Blends · Microcalorimetry · HFC · Polyaniline

Introduction

Polymer blends are synthesized to design new materials with a wide variety of properties. One of its advantages is that new materials can be synthesized from already existing materials thus reducing development cost [1]. Among polymers, polyaniline (PANI) is one of the most important conducting polymers having potentials for multitude applications, especially in electronic devices, chemical sensors, and antistatic coatings [2, 3]. One of the major disadvantages of polyaniline is its poor processability due to the rigid-rod macromolecular chains which can be improved by doping with functionalized protonic acids such as camphorsulfonic acid (CSA) [4] or dodecylbenzenesulfonic acid (DBSA) [5]. The bulky non-polar hydrophobic tail of the dopant renders the PANI soluble in non polar or weakly polar common organic solvents in which most of commercial polymers such as PVC can be codissolved. PVC is selected as an insulating polymer for blending due to its smooth surface, good flexibility, and compatibility with different additives.

Thermal properties of PANI blends have been the subject of some recent studies. Tsocheva et al. [4] reported the ageing of ethylene-co-vinyl-acetate (EVA) copolymer and PANI by using differential scanning calorimetry (DSC). Al-Ahmad et al. [6] employed thermogravimetric analysis (TG) to study the thermo-oxidative degradation of polyaniline/cellulose acetate. DSC and TG have been used to explore the thermal degradation of polyaniline–PVC blends which show that degradation of PANI proceeds by the elimination of water, loss of dopant, and eventually breakdown of polymer backbone [1, 7]. In addition to TG and DSC, isothermal heatflow microcalorimetry (HFC) can be used for life time predictions, thermal stability, oxidative degradation, and interactions between the constituents of DBSA-doped polyaniline (PANDR)/PVC blends.

HFC is adapted for continuous measurements of the heatflow that accompanies slow chemical reactions and physical processes. Due to the sensitivity of heatflow

A. B. Afzal · M. J. Akhtar (✉)
Physics Division, PINSTECH, P.O. Nilore, Islamabad 45650, Pakistan
e-mail: javeda@pinstech.org.pk; javed06@yahoo.com

A. B. Afzal
Department of Chemical and Material Engineering, PIEAS, Islamabad 45650, Pakistan

L.-G. Svensson
Bodycote Materials Testing AB, Box 431, 69127 Karlskoga, Sweden

detectors in the μW range, when combined with a high sample capacity (typically 1 g), HFC can offer up to 1,000 times higher sensitivity than a conventional DSC. The recorded raw heatflow signal is a relative measure of the reaction rate while the integrated heatflow (energy) represents a reaction parameter, i.e., the progress of the reaction. HFC has been used as a routine tool in biology and biochemistry [8]. Only a few reports are available on polymer degradation [9, 10]. In this study, HFC is employed to study the chemical stability of PANDR/PVC blends. The coupling of HFC together with FTIR can provide new information about PANDR/PVC blends.

Experimental

Synthesis of doped PANI

Aniline, ammonium peroxy disulfate (APS), and tetrahydrofuran (THF) were purchased from Riedel-de-Haën and DBSA from Fluka. Aniline was distilled under vacuum before use while all other chemicals were used as received without further purification. Deionized water was used during the experimentation.

Polyaniline doped with HCl was prepared by chemical oxidative polymerization of aniline in aqueous acidic medium (1 M HCl) using APS as an oxidant according to the procedure described by MacDiarmid et al. [11]. The reaction was carried out for ~1.5 h in the temperature range of 273–278 K. Deprotonation of the synthesized polyaniline hydrochloride was performed by treatment with 0.1 M NH_4OH. The polyaniline emeraldine base (PANIEB) so obtained was dried under dynamic vacuum for 48 h at room temperature and stored for further use.

Preparation of blends

The PANIEB powder was mechanically mixed with DBSA in an agate mortar, having PANIEB/DBSA = 1:3 (by mass) to obtain the PANDR, according to the procedure reported in the literature [12]. The solutions of PVC (5 mass%) and PANDR (2 mass%) were prepared separately in THF. The PANDR was added to the PVC solution at different proportions to prepare 5% PANDR (PANDR5), 10% PANDR (PANDR10), 15% PANDR (PANDR15), 20% PANDR (PANDR20), and 40% PANDR (PANDR40). After stirring for 2 h at room temperature, the mixed solutions were poured in the Petri dishes. The solvent was allowed to evaporate at room temperature and PANDR/PVC blend films were obtained.

In order to study the oxidation processes occurring in PANDR/PVC blends, three experiments were conducted for each PANDR5, PANDR10, PANDR15, PANDR20, and PANDR40 samples (~0.3 g) in sealed 3 cm^3 glass ampoules at 383 K. In the first experiment, the sample was saturated with oxygen gas; whereas in the second experiment nitrogen gas was flushed through the sample. The third experiment was performed in air. Thermal stability of PANDR/PVC blends was determined by measuring heatflow in an inert atmosphere like nitrogen at 383 K. In order to investigate the influence of temperature on heatflow curves of blends, the microcalorimetric measurements were carried out in sealed ampoules at different temperatures (383, 393, 403, and 413 K) in air.

Characterization

Fourier transform infrared (FTIR) spectra of blend films with varying PANDR content were recorded using Nicolet 6700 FTIR with ATR in the range of 4,000–400 cm^{-1} for 50 scans. Heatflow data of PANDR/PVC blends were obtained with a TAM III microcalorimeter from Thermometric AB, Sweden [13]. Measurements were made in the temperature range of 383–413 K. The total temperature range of the TAM III thermostat is 288 to 423 K. It can be equipped with up to 48 identical microcalorimetric units of heat conduction type in which individual experiments can be performed simultaneously. A graphical representation of an individual calorimetric unit is shown in Fig. 1. It consists of a sample and a reference sample holder symmetrically attached to a common heat sink through Peltier heat detectors for measurement of the heat exchange. The reference sample consists of an inert material with approximately the same heat capacity as the test specimen for minimization of thermal noise. The inaccuracy of the thermostat is ±0.03 K and the precision is ±0.0001 K (the certified and calibrated temperature probes were used to verify the specifications). This instrument configuration shows a short-term noise less than ±0.5 μW $(24\ h)^{-1}$ and a drift less than ±1.0 μW $(24\ h)^{-1}$. The heatflow (J s^{-1} or W) signal from the sample is a differential signal between the test and the reference ampoules, which effectively suppresses signal disturbances from temperature fluctuations in the thermostat. An internal electrical heater calibrates the calorimetric units. PANDR/PVC blend films were cut into small pieces and a mass of 0.2–0.4 g in 3 cm^3 glass ampoules was used for calorimetric experiments.

Results and discussion

FTIR

FTIR spectra of PANDR, PVC, and PANDR/PVC blends are shown in Fig. 2. The major observed peaks and their assignments are given in Table 1. The peak observed at

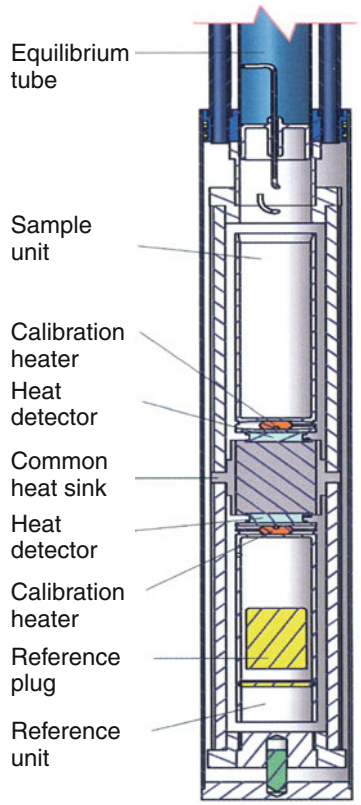

Fig. 1 A single calorimetric unit of the microcalorimeter

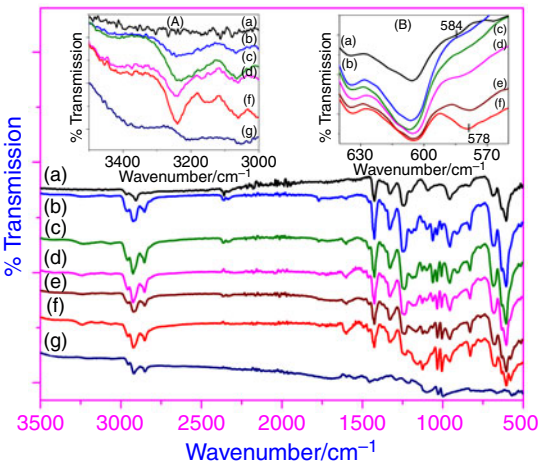

Fig. 2 FTIR spectrum of PANDR/PVC blends **a** PVC, **b** PANDR5, **c** PANDR10, **d** PANDR15, **e** PANDR20, **f** PANDR40, and **g** PANDR. Insets (*A*) and (*B*) are the N–H stretching and C–Cl stretching bands, respectively. Insets have same (**a**), (**b**), (**c**), (**d**), (**e**) and (**f**) as in the main spectrum

3,207 cm^{-1} is due to N–H stretching of amine group of PANDR as shown in inset A of Fig. 2. This peak shifts by ~32 cm^{-1} in blend which indicates that there are some sorts of interactions between PANDR and PVC. The intensity of this peak is increased as the amount of PANDR is increased. The peaks at about 1,547 and 1,455 cm^{-1} are the characteristic peaks of C=C stretching of quinoid and benzoid rings, respectively [14–16]. The presence of quinoid ring stretching indicates that dopant has been substituted in the PANI chains in all blend samples [17]. It reveals that aromatic structure of PANI is retained in all samples [18]. Two peaks near 1,028 and 998 cm^{-1} are assigned to S=O bond of DBSA and can be observed in all compositions of PANI. The band at 606 cm^{-1} corresponds to the C–Cl stretching of PVC [19]. This peak has a shoulder at 584 cm^{-1} in pure PVC (shown in inset B of Fig. 2). Mixing of PANDR in PVC shifts this shoulder peak to a lower wave number by ~6 cm^{-1}; however, intensity of this peak increases with the PANDR content. Similar results have been reported by Pan et al. [20] where it was shown that shifting of the band of carbonyl group to a lower wave number by 11 cm^{-1} in PANI/PAN (polyacrylonitrile) was due to the formation of hydrogen bond between the individual polymers. Considering the shift of N–H stretching of amine group, the shifted shoulder peaks can be attributed to the strong dipole–dipole interactions between N–H of PANDR and C–Cl of PVC.

Oxidation study

Figures 3 and 4 show the normalized heatflow as well as normalized heat energy, respectively, as a function of time for PANDR15 at 383 K. The samples in O_2 and air both respond with an instantaneous high heatflow signal upon insertion in the calorimeter. The strongly enhanced heatflow in oxygen indicates oxidation reaction in all samples. The peak heatflow of the oxygen curve increases from 239 to 2851 μW g^{-1} as the concentration of PANDR is increased from 5 to 40%. Increasing PANDR concentration also results in shorter time to heatflow maximum. The subsequent decrease in heatflow is ascribed to gradual consumption of the limited amount of O_2 available in the ampoules.

In nitrogen heatflow curve, it is observed that there is a prolonged decay extending for more than 72 h after the beginning of the measurement. Part of this weak heatflow signal and its decay can be due to the presence of traces of oxygen that are difficult to remove, e. g., due to absorption in the polymer and/or adsorption onto the ampoule walls. In addition, the signal can also contain contributions from oxygen-independent processes such as thermal degradation, interaction between the various components of the system, and crystallization etc. The same heatflow contributions of course also exist in heatflow curve measured in the presence of oxygen.

Figure 5 shows the influence of an increasing content of PANDR on the heatflow curves of blends in air at 383 K. From these results, we note that all samples show a

Table 1 Assignment of IR bands for PANDR/PVC blend films

Type of vibration	Wave number/cm^{-1}	
	PANDR	PANDR40
–N–H stretching of amine group	3,207	3,239
Aromatic C–H stretching	3,051	3,061
C–H stretching	2,953	2,962
Aromatic C–H stretching	2,919	2,924
Symmetric CH_2 stretching	2,851	2,854
Quinoid ring stretching	1,599	1,600
Benzoid ring stretching	1,455	1,425
C–H in plane bending	1,208	1,155
C–H out of plane bending	825.8	828
-S=O stretching	1,028	1,034
-S=O stretching	998	1,006
C–Cl stretching	–	605

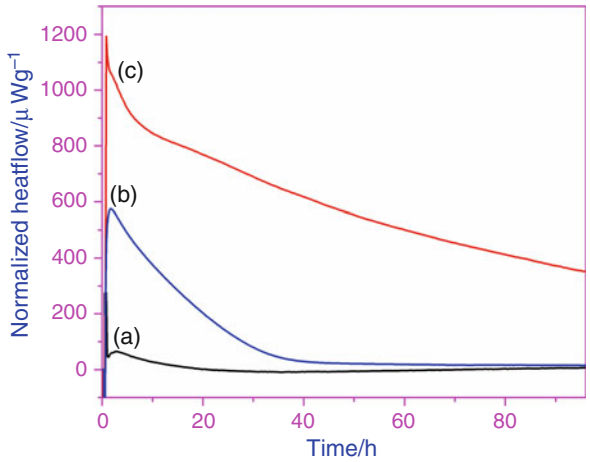

Fig. 3 Normalized heatflow versus time for PANDR15 in **a** Nitrogen, **b** Air, and **c** Oxygen at 383 K

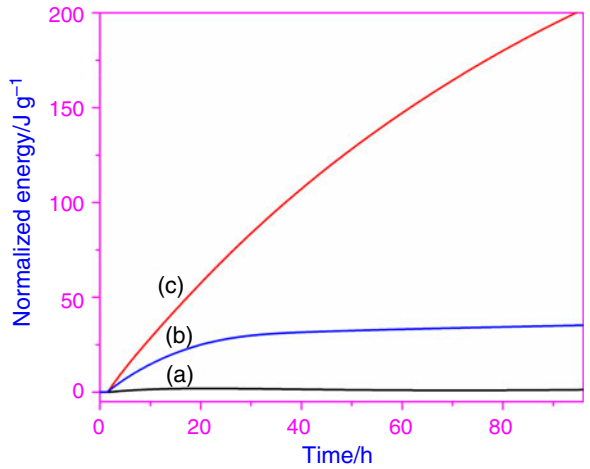

Fig. 4 Normalized energy versus time for PANDR15 in **a** Nitrogen, **b** Air, and **c** Oxygen at 383 K

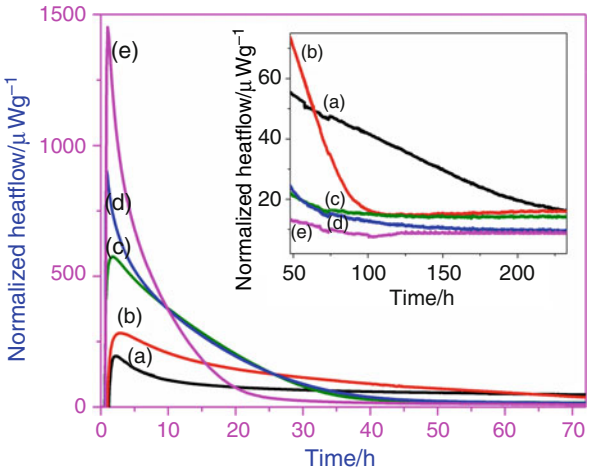

Fig. 5 Normalized heatflow versus time for **a** PANDR5, **b** PANDR10, **c** PANDR15, **d** PANDR20, and **e** PANDR40 at 383 K in air

pronounced oxidation peak after about 2 h from the time when sample ampoules are lowered in the measuring position. This peak is suppressed with increase in the content of the PVC in the blend. After consumption of the available O_2 in about 96 h, the curves return to relatively constant, non-zero levels indicating oxygen-independent chemical activity in the sample. It is well known fact that dehydrochlorination of PVC starts at about 373 K [1]. In addition to dehydrochlorination, thermal degradation of PVC polymer in the presence of oxygen also involves oxidation, with the formation of hydroperoxide, cylic peroxide, and keto groups. The evolved HCl acts as radical scavenger inhibiting the burning process [21], thus stabilizing blends with higher concentration of PVC (PANDR5) more efficiently than those with less PVC (PANDR40) in the initial part of the exotherm. As the isothermal degradation proceeds further at 383 K, the reaction of the polymer with oxygen results in deprotonation of DBSA accompanied by SO_3 substitution at the aromatic ring [22].

We can compare the heatflow levels of different samples at the same extent of reaction by plotting oxidation heatflow as a function of evolved heat energy rather than as a function of time. This technique is based on the assumption that the heat energy evolved is simply correlated to the extent of reaction [9]. In Fig. 6, the normalized heatflow is plotted as a function of normalized energy of PANDR/PVC blends at 383 K in air. It can be observed from Fig. 6 that the heatflow maximum occurs in the beginning of the reaction at low heat energy values, and that this maximum increases with decreasing PVC content. At 32 ± 4 J g^{-1}, all heatflow curves have reached very low and approximately constant levels, indicating total consumption of the O_2 available in the ampoule. The energy of oxidation, ΔH_{ox}

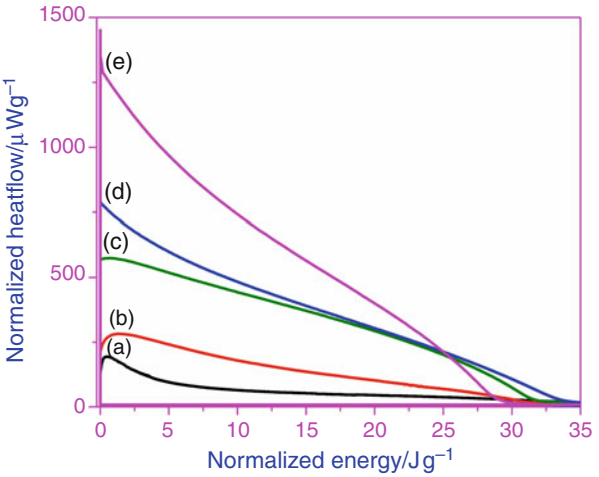

Fig. 6 Normalized heatflow versus normalized energy for **a** PANDR5, **b** PANDR10, **c** PANDR15, **d** PANDR20, and **e** PANDR40 at 383 K in air

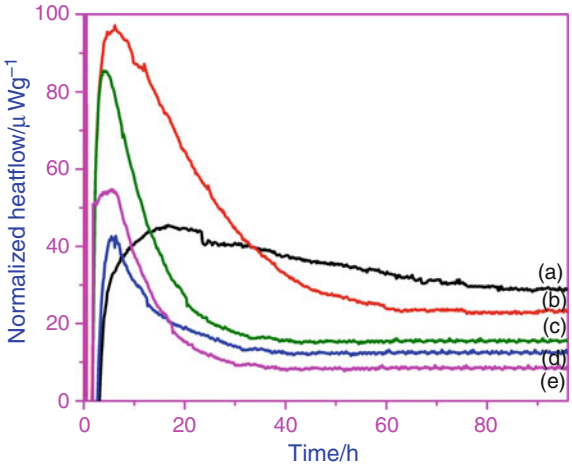

Fig. 7 Normalized heatflow versus time for **a** PANDR5, **b** PANDR10, **c** PANDR15, **d** PANDR20, and **e** PANDR40 at 383 K in nitrogen

is obviously approximately independent of the PANDR/PVC mixing ratio. Using $n \approx 2.4 \times 10^{-5}$ mol for the amount of O_2 available in ampoules with air, and $E \approx 32$ J g^{-1}; 0.3 g of sample $\approx$ 10 J we thus obtain $\Delta H_{ox} = 10/2.4 \times 10^{-5} = 417$ kJ mol^{-1} O_2.

Thermal stability beyond oxidative degradation

The plots of normalized heatflow versus time in nitrogen, as shown in Fig. 7, determine thermal stability of PANDR/PVC blends. The initial exotherm can be attributed to traces of oxygen remaining in the sample ampoule. Based on the heatflow curves, the following sequence of long-term thermal stabilities can be pointed out: PANDR40 > PANDR20 > PANDR15 > PANDR10 > PANDR5. The ratio of DBSA to PANI in PANDR is 3:1. As the concentration of PANDR is increased in the blend, the amount of the dopant is also increased. It has been already reported that doping increases the thermal stability of the conducting polymers [7, 23]; the greater thermal stability of PANDR40 is due to the presence of more acid in the blend, changing the chemical equilibrium [7]. The enhanced thermal stability of the blend with more PANDR content can be considered as an additional evidence of interactions between PANDR and PVC.

Influence of temperature

Figure 8 shows the influence of temperature on the heatflow curves of PANDR15 in air. It is observed that the curves are shifted toward longer times and lower levels at lesser temperatures. The influence of temperature on a reaction is determined by the activation energy (E_a). The relation between E_a and the rate constant (k) of a reaction is given by the Arrhenius equation:

$$k = A \cdot \exp\left(-\frac{E_a}{RT}\right) \quad (1)$$

where A is the pre-exponential factor, E_a the activation energy, R the gas constant and T the absolute temperature (K). The rate of a reaction at some natural storage temperature T_1 can be calculated from the rate at some elevated temperature T_2 by means of the acceleration factor k_T [24] defined as:

$$k_T = \exp\left[\frac{E_a}{R}\left(\frac{1}{T_1} - \frac{1}{T_2}\right)\right] \quad (2)$$

For slow reactions, activation energies can often be estimated from reaction rate data rather than directly from rate constants. In the present study, activation energies are calculated for PANDR/PVC blends by using heatflow versus heat energy plots. The advantage of using such plots is that the energy axis represents a progress parameter, here associated with the gradual reduction in oxygen concentration. Consequently, heatflow versus energy plots at different temperatures, as shown in Fig. 9, can be used to calculate the activation energy at any point along the reaction path, i.e., as a function of the degree of oxidation. Figure 10 shows such E_a versus energy curves based on the data given in Fig. 9. The curves show that E_a varies $\leq$20% over the energy range of 5–20 J g^{-1}. Samples (a), (b), and (e) show an increase in E_a with the progress of the reaction while samples (c) and (d) decrease slightly. No rational explanation can be given to this apparent lack of correlation between E_a slope and PANDR/PVC mixing ratio. Therefore, no attempt has been made to interpret the

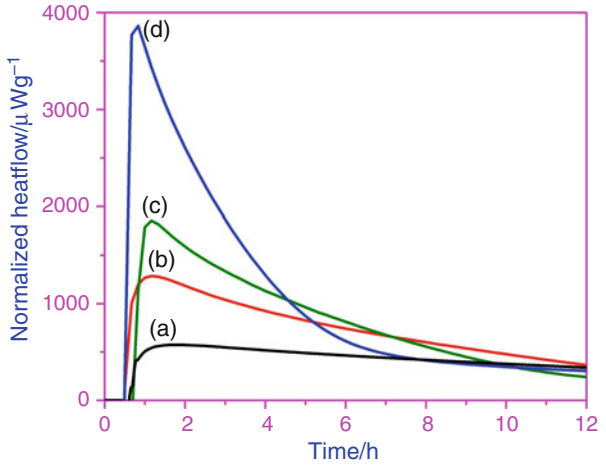

Fig. 8 Normalized heatflow versus time for PANDR15 at **a** 383 K, **b** 393 K, **c** 403 K, and **d** 413 K in air

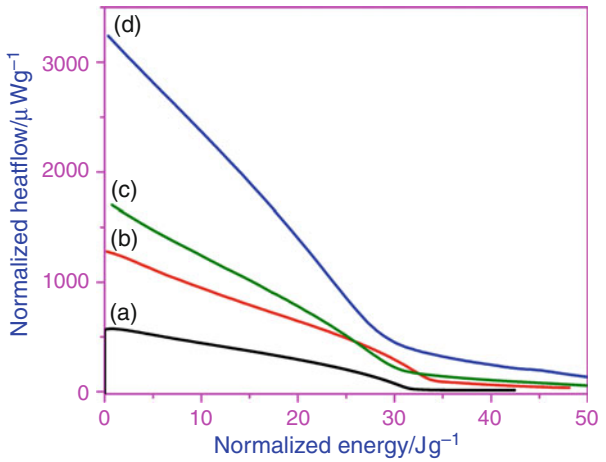

Fig. 9 Normalized heatflow versus normalized energy for PANDR15 at **a** 383 K, **b** 393 K, **c** 403 K, and **d** 413 K in air

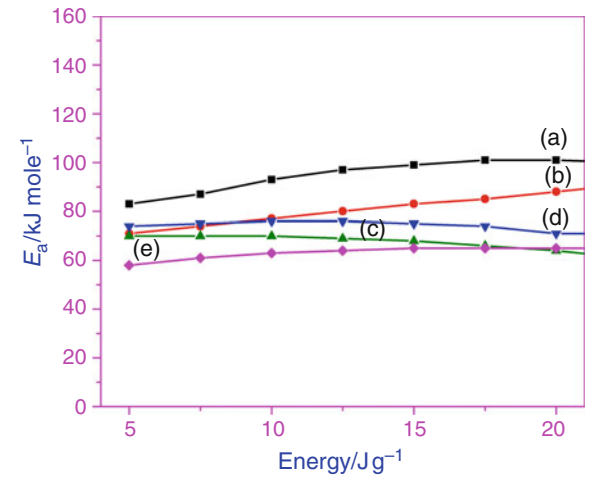

Fig. 10 E_a versus normalized energy for **a** PANDR5, **b** PANDR10, **c** PANDR15, **d** PANDR20 and **e** PANDR40

variation in E_a in terms of possible changes in the oxidation reaction mechanisms along the reaction path.

Activation energies and acceleration factors for all samples, evaluated at $E = 5$ J g^{-1}, are summarized in Table 2. We note that PANDR40 has lower activation energy than PANDR5, despite the fact that it is the more stable. It can thus be concluded that there is no direct relationship between activation energy and thermal stability of PANDR/PVC blends [7].

Representative examples of Arrhenius plots are given in Fig. 11, based on heatflow values at $E = 5$ J g^{-1}. The plots show acceptably good linearity. Using Eq. 2 with natural storage temperature $T_1 = 298$ K (25 °C) and accelerated temperature $T_2 = 343$ K (70 °C) yields the acceleration factors listed in Table 2. For example, 1 h at 343 K simulates 41 h at 298 K for PANDR15. Such information can be useful for the design of temperature-accelerated ageing of PANDR/PVC blends.

Degradation study

In a blend having two components such as PVC and PANDR, it is possible to estimate the degradation of each component, either by considering that all energy is contributed by one component (worst case calculation) or by combining energy data for the samples with different PVC/PANDR mixing ratios to obtain discrete energy contributions from each component. The latter approach has been used in this study. The following equation is used to convert energy to % degradation of the respective component (X) of the blend:

$$\%\ \text{degradation of X} = \frac{100 \cdot E(t_o).M_X}{\Delta H_X \cdot S_X} \tag{3}$$

here $E(t_o)$ is the total energy (J g^{-1} of sample) released at time t_o, M_x the molecular mass (g mol^{-1} of repeating unit in the polymer), ΔH_x the degradation reaction enthalpy (J mol^{-1}), and S_X the number of reactive sites per repeating unit, respectively.

Table 2 Kinetic parameters calculated for oxidation of PAND/PVC blends using isothermal calorimetric data at 413 K

Samples	A	K	E_a/kJ mol^{-1}	k_T
PANDR5	7.19 × 1,012	547	83	81
PANDR10	1.36 × 1,015	1,314	71	43
PANDR15	2.01 × 1,012	2,810	70	41
PANDR20	1.06 × 1,013	3,475	74	50
PANDR40	2.07 × 1,013	3,784	58	22

A is the pre-exponential factor, k the rate constant, E_a the activation energy and k_T, the acceleration factor, for simulation at 343 K. All values are based on heatflow data for $E = 5$ J g^{-1}

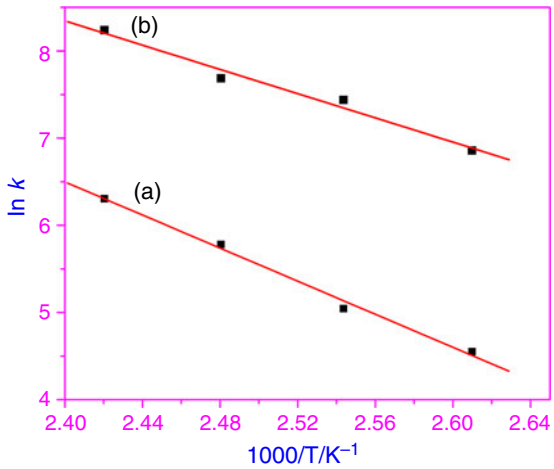

Fig. 11 Arrhenius plots for **a** PANDR5, and **b** PANDR40

Realistic values can normally be assigned to M_X and S_X provided that the chemistry of the degradation reaction is known. ΔH_x can theoretically be calculated from reactants and reaction products by means of Hess' law, provided that all products are known. Crude ΔH_x values can be used for rough estimations of sample degradation. This approach has been employed for calculation of the % degradation of PANDR and PVC after 72 h of reaction at 413 K; these results are summarized in Table 3.

The degradation data presented in Table 3 are derived using the following model. The energy is assumed to consist of discrete contributions from PANDR (E_1) and PVC (E_2), i.e.,

$$E = \alpha_1 E_1 + \alpha_2 E_2 \quad (4)$$

where α_1 and α_2 denote the mass fraction of PANDR and PVC, respectively. Since energy data are available for five different mixing ratios (40, 51.2, 53.3, 64.5, and 89.9 J g^{-1} for 5, 10, 15, 20, and 40% addition of PANDR in PVC, respectively) we have a system of five equations but only two unknown (E_1, E_2). All ten possible combinations of two of these five equations have been used to calculate the average values of E_1 and E_2 in Table 3. Despite quite a large scattering in the results from the 10 calculations, as indicated by the standard deviation, it is obvious that the major part of the energy is associated with the ageing of PANDR. Insertion of the energy values into Eq. 3 yields the approximate degradation percentage given in Table 3.

Table 3 % degradation of individual components of PANDR/PVC blends after 72 h at 413 K

Component	Energy (average)/J g^{-1}	Energy (SD)/J g^{-1}	Degradation (average)/%
PANDR	180	45	10
PVC	34	7	2

The results are based on the following assumptions: For PANDR degradation: $\Delta H_x = 100$ kJ mol^{-1}, $M_x = 334$ g mol^{-1}, $S_x = 6$. For PVC degradation: $\Delta H_x = 100$ kJ mol^{-1}, $M_x = 62.5$ g mol^{-1}, $S_x = 1$

The ageing of PANDR involves the removal of doped acid, which in the presence of oxygen stimulates the fragmentation and sulfonation of PANI backbone, leading to chemical cross-linking by formation of interchain tertiary amine bonds [22]. Whereas, thermo-oxidative degradation of PVC involves the formation of HCl, hydroperoxide, aldehydes, ketones, alcohols, carboxylic acid, and carbon monoxide. The chain propagation involves an exclusive attack of peroxy radicals on the hydrogen of chloromethylene groups. As indicated in Table 3, the degradation of PANDR is likely to be higher than for PVC. In PANDR the DBSA, acting as a dopant, is attached to the PANI backbone through physical interactions and can easily be removed upon heating at higher temperature thus further degrading the polymer. However, PVC is the stable one due to the presence of covalent bonds.

Compatibility analysis

Compatibility refers to the mutual interactions between two or several different substances. In the PANDR/PVC blends, the major reaction is the oxidation reactions as described earlier. The PANDR and PVC components of the blend are not separated in the film form but there exists some mutual interactions between them. Without such interaction the normalized energy of a PVC/PANDR mixture would simply equal the weighted average of the pure PVC and PANDR normalized energies. The interaction energy (E_{int}) which is the difference in heat between an experimental mixture curve and the corresponding weighted average of the pure components is a measure of chemical interaction [25, 26]. According to Fig. 12, the so-called

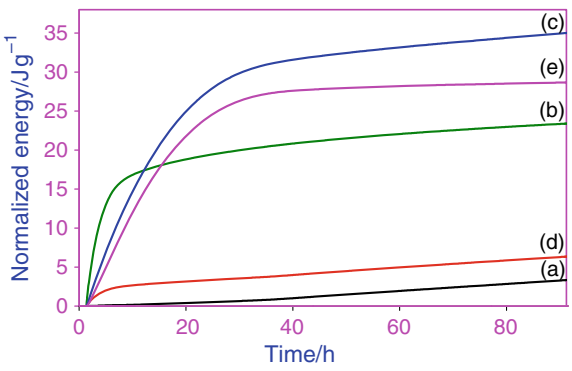

Fig. 12 Normalized energy versus time for **a** PVC, **b** PANDR, **c** PANDR15, **d** non-interaction curve, and **e** interaction curve at 383 K in air

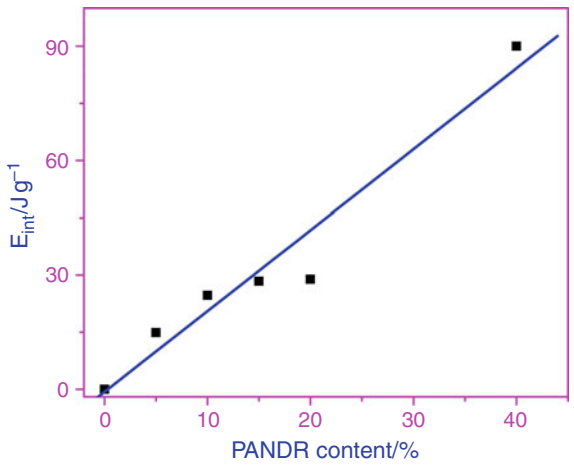

Fig. 13 Interaction energy versus PANDR content at normalized energy of 3 J g^{-1}

non-interaction energy (d) amounts to 5.5 J g^{-1} after 72 h, while the actual energy for the blend film containing 85% PVC and 15% PANDR (c) is 34 J g^{-1}.

Interaction energies have been calculated for all five PVC/PANDR blends; these results are plotted as a function of PANDR content in Fig. 13. It can be observed that the interaction energy increases by increasing PANDR concentration in the blend. Linear regression has been used to fit a straight line to the data points in Fig. 13. By means of the slope E_{int} can be normalized to approximately 2.1 J per % of PANDR.

The experimentally obtained difference in energy of the pure PVC (a) and PANDR (b) components in Fig. 12 conforms acceptably well on a relative scale with the energy difference, given in Table 3, calculated from samples with various PVC/PANDR ratios. It shall be emphasized that the calculation model presented in Table 3 does not make any assumptions concerning reaction mechanisms—including PVC/PANDR interactions. It just formally assigns energy values to the respective component on a purely mathematical basis. The actual reason why the oxidation heatflow increases relative to the heatflow from each separate component is currently unknown. It can be a purely chemical interaction effect, but it is also possible that physical effects such as increased oxygen accessibility to reactive sites through changes in the polymer chain mobility can play a role.

Conclusions

The PANDR/PVC blends were synthesized by solution blending technique. FTIR confirmed the doping of PANI by DBSA and showed that there exist strong dipole–dipole interactions between individual components of the blends. The energy of oxidation is independent of the PANDR/PVC mixing ratio. The thermal stability of the blends increased with PANDR content. The activation energies, determined from the slope of Arrhenius plots, provide information about acceleration factors which can be used for temperature-accelerated ageing of blends. The average degradation of PANDR is higher than that of PVC. The compatibility analysis indicated that the interaction between individual components increased by increasing the PANDR content in the blend.

Acknowledgements We are grateful to Higher Education Commission (HEC) of Pakistan for the financial support through indigenous scholarship scheme for Ph. D. studies of Asma Binat Afzal in science and technology (Batch II). We are thankful to Dr. Dan Forsström for his help in the experiment and useful discussions.

References

1. Pielichowski K. Thermal degradation of poly(vinyl chloride)/polyaniline conducting blends. J Therm Anal Calorim. 1998;54:171–5.
2. Gul VE. Structure and properties of conducting polymer composites. Utrecht, The Netherlands: VSP; 1996.
3. Shipway AN, Willner I. Nanoparticles as structural and functional units in surface-confined architectures. Chem Commun. 2001;2035–45.
4. Tsocheva D, Tsanov T, Terlemezyan L. Ageing of conductive Polyaniline/poly(ethylene-co-vinylacetate) composites studied by thermal methods. J Therm Anal Calorim. 2002;68:159–68.
5. Cao Y, Smith P, Heeger AJ. Counter-ion induced processability of conducting polyaniline and of conducting polyblends of polyaniline in bulk polymers. Synth Met. 1992;48:91–7.
6. Al-Ahmed A, Mohammad F, Rahman MZA. Composites of polyaniline and cellulose acetate: preparation, characterization, thermo-oxidative degradation and stability in terms of DC electrical conductivity retention. Synth Met. 2004;144:29–49.
7. De Farias RF, Nunes LM. Thermogravimetric study about PVC-polyaniline blends. J Therm Anal Calorim. 2002;70:559–64.
8. Lin FY, Chen WY, Hearn M. Microcalorimetric studies on the interaction mechanism between proteins and hydrophobic solid surfaces in hydrophobic interaction chromatography: effects of salt, hydrophobicity of the sorbent, and structure of the protein. Anal Chem. 2001;73:3875–83.
9. Forsstrom D, Svensson LG, Terselius B. Thermo-oxidative stability of polyamide 6 films III. Isothermal microcalorimetry. Polym Deg Stab. 2000;67:263–9.
10. Forsstrom D, Hamskog M, Eriksson P, Terselius B. Oxidation of unstabilised polypropylene particles as studied by microcalorimetry and chemiluminescence techniques. Polym Deg Stab. 2003;81:81–8.
11. MacDiarmid AG, Chiang JC, Richter AF, Somasiri NLD, Epstein AJ. Polyaniline: Synthesis and characterization of the emeraldine oxidation state by elemental analysis. In: Alcacer L, editor. Conducting polymers. Dordrecht: Reidel Publishing Co; 1987. p. 105–20.
12. Cao Y, Smith P, Heeger AJ. Counter-ion induced processibility of conducting polyaniline. Synth Met. 1993;57:3514–9.
13. Suurkuusk J, Wadso I. A multichannel microcalorimetry system. Chem Scr. 1982;20:155–63.

14. Afzal AB, Akhtar MJ, Nadeem M, Ahmed M, Hassan MM, Yasin T, Mehmood M. Structural and electrical properties of polyaniline/silver nanocomposites. J Phys D Appl Phys. 2009;42:015411 (8 pp).
15. Afzal AB, Akhtar MJ, Nadeem M, Hassan MM. Investigation of structural and electrical properties of polyaniline/gold nanocomposites. J Phys Chem C. 2009;113:17560–5.
16. Afzal AB, Akhtar MJ, Nadeem M, Hassan MM. Dielectric and impedance studies of DBSA doped polyaniline/PVC composites. Curr Appl Phys 2010;10:601–6.
17. Ameen S, Ali V, Zulfequar M, Haq MM, Husain M. Electrical and spectroscopic characterization of polyaniline-polyvinyl chloride (PANI-PVC) blends doped with sodium thiosulphate. Physica B Condens Matter. 2008;403:2861–6.
18. Cui B, Qiu H, Fang K, Fang C. Effect of vacuum annealing on characteristics of the DBSA-doped polyaniline pellets. Synth Met. 2007;157:11–6.
19. Beltran M, Marcilla A. Fourier transform infrared spectroscopy applied to the study of PVC decomposition. Eur Polym J. 1997;33:1135–42.
20. Pan W, Yang SL, Li G, Jiang JM. Electrical and structural analysis of conductive polyaniline/polyacrylonitrile composites. Eur Polym J. 2005;41:2127–33.
21. Pielichowski K, Janowski B. Semi-interpenetrating polymer networks of polyurethane and poly(vinyl chloride). J Therm Anal Calorim. 2005;80:147–51.
22. Rannou P, Nechtschein M, Travers JP, Berner D, Wolter A, Djurado D. Ageing of PANI: chemical, structural and transport consequences. Synth Met. 1999;101:734–7.
23. Neoh KG, Kang ET, Tan KL. Thermal degradation of leucoemeraldine, emeraldine base and their complexes. Thermochim Acta 1990;171:279–91.
24. Svensson LG. Using isothermal microcalorimetry for the prediction and testing of long-term properties of materials and products. J Therm Anal Calorim. 1997;49:1017–23.
25. Elmqvist CJ, Lagerkvist PE, Svensson LG. Stability and compatibility testing using a microcalorimetric method. J Hazard Mater. 1983;7:281–90.
26. Svensson LG, Taylor DE, Forsgren CK, Backman PO. Microcalorimetry and impact testing applied to the study of explosive/polymer compatibility. In: Proceedings of ADPA symposium on compatibility of plastics and other materials with explos propell pyrot. Long Beach, California, USA; 1986, p. 86–91.